the plant journal

SEB Society for Experimental Biology

The Plant Journal (2015) **82,** 925–936 doi: 10.1111/tpj.12868

Regulation of flowering time by the histone deacetylase HDA5 in Arabidopsis

Ming Luo[1,2,†], Ready Tai[2,†], Chun-Wei Yu[2,†], Songguang Yang[1], Chia-Yang Chen[2], Wen-Dar Lin[3], Wolfgang Schmidt[3] and Keqiang Wu[2,*]

[1]*Key Laboratory of South China Agricultural Plant Molecular Analysis and Genetic Improvement, South China Botanical Garden, Chinese Academy of Sciences, No. 723, Xingke Road, 510650 Guangzhou, China,*

[2]*Institute of Plant Biology, College of Life Science, National Taiwan University, No. 1, Sec. 4, Roosevelt Road, 10617 Taipei, Taiwan, and*

[3]*Institute of Plant and Microbial Biology, Academia Sinica, No. 128, Sec. 2, Academia Road, 11529 Taipei, Taiwan*

Received 28 July 2014; revised 30 March 2015; accepted 15 April 2015; published online 29 April 2015.
*For correspondence (email: kewu@ntu.edu.tw).
†These authors contributed equally to this work.

SUMMARY

The acetylation level of histones on lysine residues regulated by histone acetyltransferases and histone deacetylases plays an important but under-studied role in the control of gene expression in plants. With the aim of characterizing the Arabidopsis RPD3/HDA1 family histone deacetylase HDA5, we present evidence showing that HDA5 displays deacetylase activity. Mutants defective in the expression of *HDA5* displayed a late-flowering phenotype. Expression of the flowering repressor genes *FLC* and *MAF1* was up-regulated in *hda5* mutants. Furthermore, the gene activation markers, histone H3 acetylation and H3K4 trimethylation on *FLC* and *MAF1* chromatin were increased in *hda5-1* mutants. Chromatin immunoprecipitation analysis showed that HDA5 binds to the chromatin of *FLC* and *MAF1*. Bimolecular fluorescence complementation assays and co-immunoprecipitation assays showed that HDA5 interacts with FVE, FLD and HDA6, indicating that these proteins are present in a protein complex involved in the regulation of flowering time. Comparing gene expression profiles of *hda5* and *hda6* mutants by RNA-seq revealed that HDA5 and HDA6 co-regulate gene expression in multiple development processes and pathways.

Keywords: Arabidopsis, flowering, HDA5, HDA6, histone deacetylase.

INTRODUCTION

In eukaryotes, epigenetic mechanisms including histone modifications and DNA methylation play a crucial role in the regulation of gene expression. Histone modifications such as acetylation, methylation, ubiquitination, sumoylation, phosphorylation and ADP ribosylation directly affect histone structure and/or provide interaction sites for other chromatin-associated factors (Berger, 2007). All of these modifications are reversible and are maintained by various histone-modifying enzymes. The levels of histone acetylation are regulated by histone acetyltransferases and histone deacetylases (HDACs or HDAs) (Liu *et al.*, 2014). In general, hypoacetylated histones are associated with gene repression, whereas hyperacetylated histones are related to gene activation.

HDACs in all eukaryotes may be grouped into three families: RPD3/HDA1 (Reduced Potassium Dependence 3/Histone Deacetylase 1), SIR2 (Silent Information Regulator 2) and HD2 (Histone Deacetylase 2) (Yang and Seto, 2007; Liu *et al.*, 2014). The Arabidopsis RPD3/HDA1 family HDACs may be further divided into three classes. Class I includes HDA19, HDA6, HDA7 and HDA9; class II includes HDA5, HDA15 and HDA18; class III includes HDA2 only (Hollender and Liu, 2008; Alinsug *et al.*, 2009). Most studies on plant HDACs have focused on the class I HDACs HDA6 and HDA19. The *HDA6* mutants *axe1* and *rst1* exhibit increased expression of transgenes and reduced DNA methylation, indicating that HDA6 is involved in gene silencing and DNA methylation (Aufsatz *et al.*, 2002; To *et al.*, 2011; Liu *et al.*, 2012). Furthermore, HDA6 is also involved in the regulation of flowering time and leaf development (Yu *et al.*, 2011; Luo *et al.*, 2012). HDA19 has been associated with various developmental processes such as flowering, floral organ identity, seed development and circadian clocks (Tian and Chen, 2001; Long *et al.*, 2006; Krogan *et al.*,

2012; Wang *et al.*, 2013; Zhou *et al.*, 2013). Recent studies indicated that HDA6 and HDA19 are recruited by various transcriptional factors and form multiple protein complexes that are involved in various developmental proecess in plants (Liu *et al.*, 2014).

In Arabidopsis, flowering time is controlled by several flowering-promoting pathways, including vernalization, autonomous, photoperiod and gibberellin pathways (Henderson and Dean, 2004). *FLOWERING LOCUS C* (*FLC*), encoding a MADS box domain transcription factor, functions as a key repressor gene in flowering. A number of studies have demonstrated that transcription regulation of *FLC* is modulated by both genetic and epigenetic mechanisms. *FLC* expression is positively regulated by FRIGIDA (FRI) and FRI-like proteins (Michaels and Amasino, 1999; Michaels *et al.*, 2004). In contrast, expression of *FLC* is negatively regulated by genes in the autonomous pathway, such as *FLOWERING LOCUS D* (*FLD*), *FVE* and *FCA* (He *et al.*, 2003; Ausin *et al.*, 2004; Liu *et al.*, 2007). FLD is a lysine-specific demethylase 1-type histone demethylase involved in the demethylation and deacetylation lysine 4 of histone H3 in *FLC* chromatin (He *et al.*, 2003; Jiang *et al.*, 2007; Liu *et al.*, 2007; Yu *et al.*, 2011). Similarly, FCA and FVE also participate in demethylation and deacetylation lysine 4 of histone H3 in *FLC* chromatin (He *et al.*, 2003; Ausin *et al.*, 2004; Liu *et al.*, 2007). Mutations of these genes cause high expression of *FLC* and delayed flowering. More recently, it was demonstrated that the autonomous pathway represses *FLC* expression through antisense RNA-mediated chromatin modifications (Liu *et al.*, 2007; letswaart *et al.*, 2012; Marquardt *et al.*, 2014; Wang *et al.*, 2014). In the absence of FCA, the *COOLAIR* transcript is polyadenylated at a distal poly(A) site. This is associated with high H3K4me2 levels in *FLC* chromatin as well as high levels of functional *FLC* mRNA and *COOLAIR* expression. FCA promotes alternative polyadenylation of *COOLAIR* by targeting FY activity to a proximal poly(A) site. This event is likely to trigger FLD-dependent demethylation in *FLC* chromatin, leading to a transcriptionally repressed state and low levels of functional *FLC* mRNA (Liu *et al.*, 2007, 2010).

HDA6 regulates flowering time by directly interacting with FLD (Yu *et al.*, 2011). Increased levels of histone H3 acetylation and H3K4 trimethylation at *FLC*, the key repressor of flowering, were found in both *hda6* and *fld* mutant plants, suggesting that both HDA6 and FLD are involved in gene regulation by histone deacetylation and demethylation. Furthermore, HDA6 was also shown to associate with FVE/MSI4, the Arabidopsis homolog of the human histone-binding proteins RbAp46/48, for repression of *FLC* expression (Gu *et al.*, 2011). Collectively, these data suggest that HDA6 may form a HDAC complex with FVE and FLD to regulate gene expression for control of flowering time.

In the present study, we found that the Arabidopsis class II HDAC HDA5 is involved in the regulation of flowering time by repressing *FLC* and *MAF1* expression. Furthermore, HDA5 and HDA6 form a HDAC complex with FLD and FVE to regulate gene expression to control flowering time in Arabidopsis.

RESULTS

HDA5 displays histone deacetylase activity

We investigated the deacetylase activity of the Arabidopsis RPD3/HDA1 proteins HDA2, HDA5, HDA6, HDA9, HDA15 and HDA18. The full-length cDNAs of *hda* genes were inserted into the pGEX4T-3 vector to create N-terminal glutathione-*S*-transferase (GST) fusions. The recombinant GST–HDA proteins were expressed in *Escherichia coli* Rosetta, and purified by affinity column purification using GST resins. The GST–HDA recombinant proteins were incubated with a fluorogenic peptidic HDAC substrate containing an ε-acetylated lysyl moiety. A HeLa nuclear extract containing a mixture of HDACs served as a positive control, and the HDAC inhibitor trichostatin A (TSA) was used to demonstrate the specificity of deacetylation activities. As shown in Figure 1b, GST–HDA5 showed histone deacetylase activity. In contrast, recombinant proteins of HDA6 (Figure 1b) and other HDACs, including GST–HDA2, GST–HDA9, GST–HDA15 and GST–HDA18, produced in *E. coli* did not show measurable histone deacetylase activity.

X-ray crystal structures of human HDACs revealed that HDACs are typically Zn^{2+}-containing enzymes (Vannini *et al.*, 2004). In human HDAC8, three amino acids (D178, H180 and D267) are responsible for chelating Zn^{2+}. These three amino acids are conserved in Arabidopsis HDA5, corresponding to D198, H200 and D291 (Figure 1a). In human HDAC8, mutations on each of these three amino acids affects the structure for binding substrates and therefore completely abolishes the enzymatic activity (Vannini *et al.*, 2004). Similarly, the mutant recombinant proteins GST–HDA5_D198A, GST–HDA5_D291A and GST–HDA5_H200A, in which the conserved amino acids have been replaced by alanine, did not show histone deacetylase activity (Figure 1b). These data indicate that D198, D291 and H200 are required for HDA5 activity and may also be responsible for metal chelating.

We further purified GFP-tagged HDA5 from transgenic Arabidopsis plants expressing the GFP–*HDA5* chimeric gene driven by the CaMV 35S promoter. As shown in Figure 1c, purified GFP–HDA5 protein from transgenic plants also displayed HDAC activity, and this activity was inhibited by TSA. Taken together, our data demonstrated that HDA5 is a histone deacetylase with enzymatic activity.

hda5 mutants display delayed flowering

To investigate the biological function of HDA5, we identified two *HDA5* mutant lines, *hda5-1* (SALK_007503) and *hda5-2* (SALK_021241). *hda5-1* and *hda5-2* mutant lines carry T-DNA insertions in the 12th and 1st introns of *HDA5*, respectively

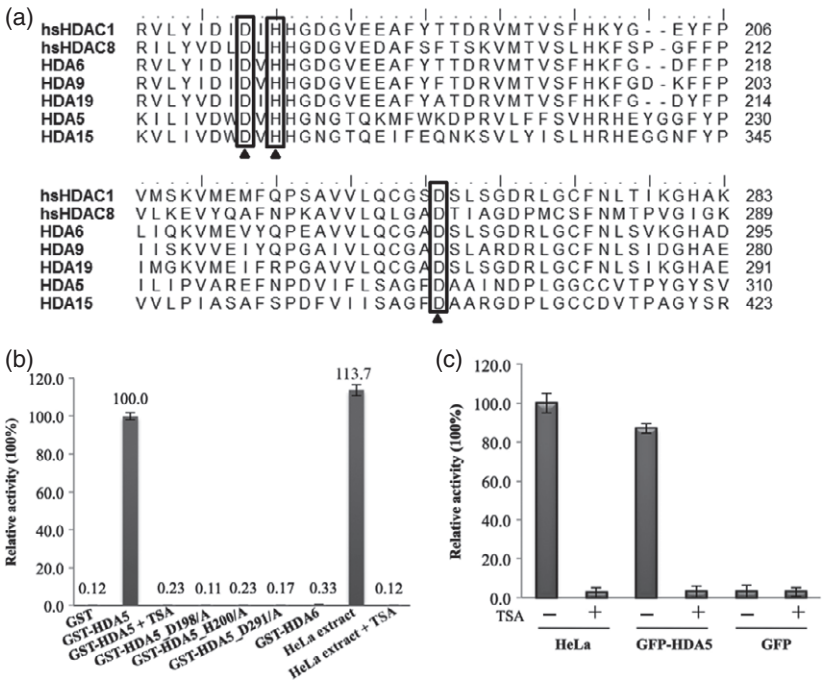

Figure 1. HDA5 displays histone deacetylase activity.

(a) Alignment of the conserved catalytic domains of human HDAC1 (hsHDAC1) and hsHDAC8 with those of Arabidopsis HDA5, HDA6, HDA9, HDA15 and HDA19. The arrowheads and boxes indicate three conserved amino acids that are responsible for chelating Zn^{2+} in hsHDAC8.

(b) Histone deacetylase activity of GST–HDA5 recombinant proteins treated with or without TSA (0.1 mM). *In vitro* activity of HDA5 was totally abolished when any of the three conserved amino acids was mutated. A nuclear extract from HeLa cells and GST protein alone were used as the positive and negative controls, respectively.

(c) Deacetylase activity of purified GFP–HDA5 from transgenic Arabidopsis plants.

(Figure 2a). Homozygous *hda5-1* and *hda5-2* lines were identified by PCR assays (Figure 2b). Compared to wild-type Col plants, *HDA5* transcript was absent in *hda5-1* mutant plants and showed markedly lower abundance in *hda5-2* mutant plants (Figure 2c), indicating that *hda5-1* is a knockout mutant line whereas *hda5-2* is a knockdown mutant line.

Delayed-flowering phenotypes were observed in both *hda5-1* and *hda5-2* mutant plants (Figure 3). As our previous studies demonstrated that the *hda6* mutant, *axe1-5*, also displayed a delayed-flowering phenotype (Yu *et al.*, 2011), we compared the rosette leaf numbers and day of bolting for *hda5* and *hda6* (*axe1-5*) mutant lines under both long-day conditions (LD, 16 h light/8 h dark) and short-day conditions (SD, 8 h light/16 h dark). The flowering time of *hda5-1*, *hda5-2* and *hda6* plants was greatly delayed under LD as well as SD conditions in terms of both the number of days to flowering and the number of rosette leaves at bolting (Figure 3a,b). In addition, the delay in flowering time of *hda5* and *hda6* plants was completely corrected by 45 days of vernalization at 4°C (Figure 3c), indicating that HDA5 and HDA6 are involved in the autonomous flowering pathway. We also analyzed *hda5-1*/*fve* double mutants. *hda5-1*/*fve* double mutants flowered later than *hda5-1* and *fve* single mutants (Figure S1), suggesting that, in addition to HDA5, other HDAs such as HDA6 are also involved in the autonomous flowering pathway.

The expression of FLC *and* MAF1 *is increased in* hda5 *mutants*

FLC is a key transcriptional repressor that controls the transition from vegetative to reproductive development (Michaels and Amasino, 2001). We collected plant samples grown under LD conditions for 15 days, and examined the mRNA level of *FLC* in *hda5* and *hda6* mutant plants. As shown in Figure 4a, the expression of *FLC* was up-regulated in *hda5* and *hda6* mutant plants. Recent studies indicated that the *FLC* clade members MAF1–MAF5 may form a repressor complex and function redundantly in controlling flowering time (Scortecci *et al.*, 2001; Ratcliffe *et al.*, 2003; Gu *et al.*, 2013). We thus also measured the expression of *MAF1–MAF5* in *hda5* and *hda6* mutant plants. The expression of *MAF1* was significantly increased in *hda5* and *hda6* mutants compared to wild-type plants (Figure 4a). In contrast, the transcript levels of *MAF4* and *MAF5* were significant increased in *hda6* plants but not in *hda5* plants. In addition, the transcript levels of two downstream flowering integrators, *FT* and *SOC1*, were decreased in both *hda5* and *hda6* mutant plants (Figure 4b).

To investigate whether the delayed-flowering phenotype of *hda5* mutant is dependent on *FLC* and *MAF1* expression, we generated *hda5-1*/*flc-3* and *hda5-1*/*maf1-2* double mutants. *hda5-1*/*flc-3* and *hda5-1*/*maf1-2* double mutant plants flowered earlier than *hda5-1* plants (Figure S2), indicating that the late-flowering phenotype of *hda5-1* is indeed FLC- and MAF1-dependent.

HDA5 binds to FLC *and* MAF1 *chromatin*

To examine whether HDA5 binds to *FLC* and *MAF1* chromatin directly, transgenic plants expressing TAP-tagged *HDA5* driven by the CaMV 35S promoter were generated (Rubio *et al.*, 2005). Over-expression of *HDA5–TAP* in *hda5-*

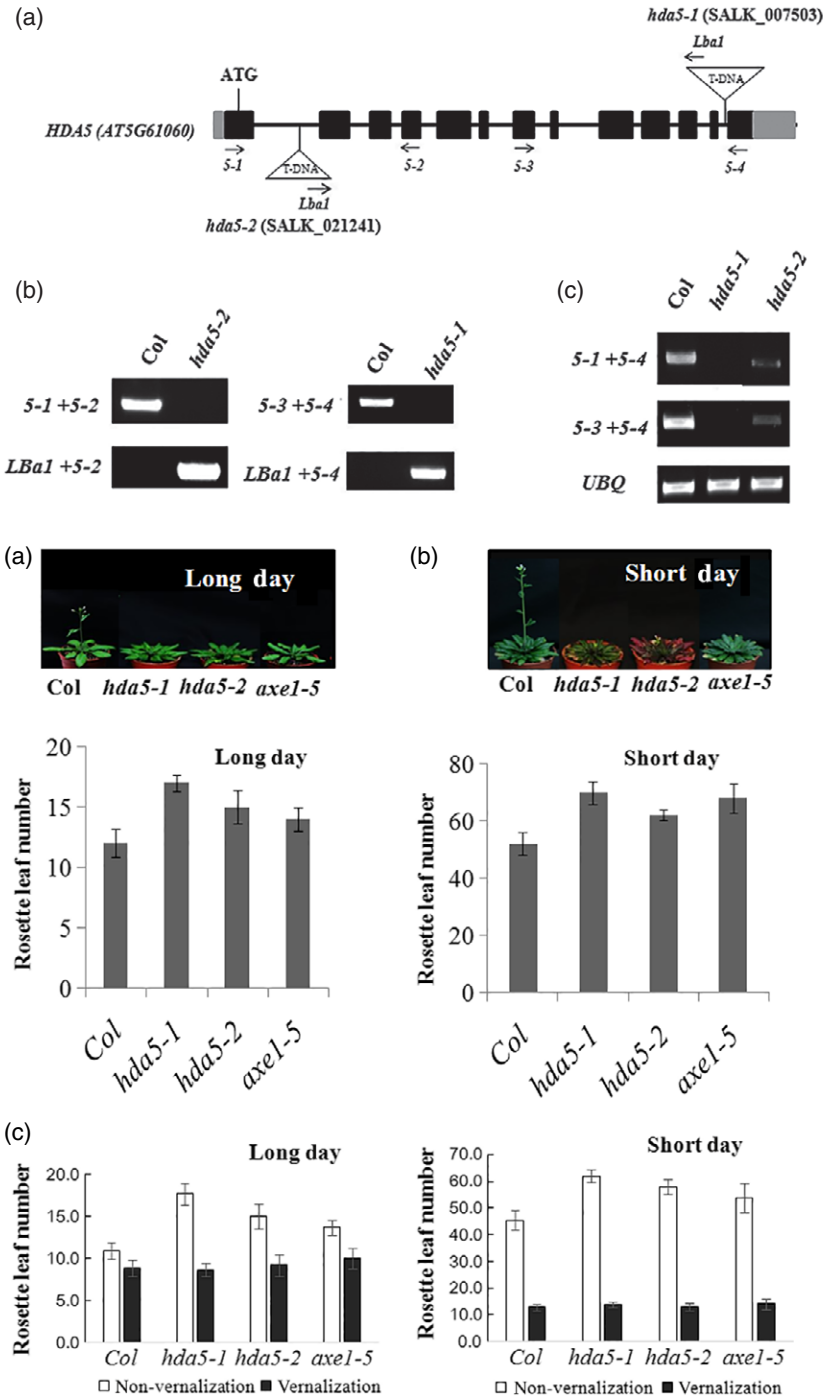

Figure 2. Identification of the T-DNA mutants of *HDA5*.
(a) The positions of the T-DNA insertions (SALK_007503 and SALK_021241) and primers used for PCR amplification in the *HDA5* locus. Exons and untranslated regions are represented by black and gray boxes; introns are represented by black lines.
(b) PCR-based screen showing that both *hda5-1* and *hda5-2* are homozygous mutant lines.
(c) RT-PCR showing that HDA5 transcript is absent in *hda5-1* plants but down-regulated in *hda5-2* plants. *UBIQUITIN10* (*UBQ*) was used as an internal control.

Figure 3. Delayed-flowering phenotypes of *hda5* mutants.
(a,b) Delayed-flowering phenotypes of *hda5-1*, *hda5-2* and *axe1-5* mutants under long-day (LD) and short-day (SD) conditions.
(c) Phenotype of *hda5-1*, *hda5-2* and *axe1-5* mutants with or without vernalization treated under LD or SD conditions. Rosette leaf numbers were determined from at least 20 plants for each line. Values are means ± SD.

1 complemented the delayed-flowering phenotype (Figure S3), suggesting that the HDA5–TAP protein is functional *in vivo*. Chromatin immunoprecipitation (ChIP) assays using anti-Myc antibody revealed that HDA5 bound to the promoters and first exons of *FLC* and *MAF1* (Figure 5), indicating that HDA5 directly binds to *FLC* and *MAF1* and represses their expression in Arabidopsis. For comparison, ChIP assays revealed that HDA6 bound to *FLC*, *MAF1*, *MAF4* and *MAF5* (Figure S4).

We further investigated whether the high expression of *FLC* and *MAF1* in *hda5* mutants was correlated with increased histone acetylation levels in chromatin. ChIP assays were performed, and the relative enrichment of histone H3 lysine 9 and lysine 14 acetylation (H3K9K14Ac) was examined by quantitative real-time PCR. As shown in Figure 6a, hyperacetylation of histone H3K9K14 was found in the promoter, first exon and first intron regions of *FLC* and *MAF1* in *hda5-1* mutants, suggesting that HDA5 may

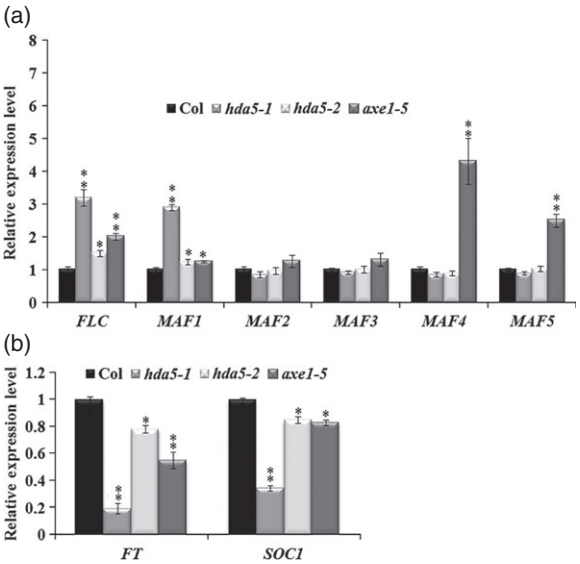

Figure 4. Expression levels of flowering genes in *hda5* and *hda6* mutants.
(a) Relative expression of *FLC* clade members in *hda5-1*, *hda5-2* and *axe1-5* mutants.
(b) Relative expression of *FT* and *SOC1* in *hda5-1*, *hda5-2* and *axe1-5* mutants. RNA was extracted from plants grown under LD conditions for 15 days.

regulate *FLC* and *MAF1* expression through histone deacetylation.

The level of histone H3 lysine 4 trimethylation (H3K4Me3) was also investigated in *hda5-1* mutant plants. Increased levels of H3K4Me3 were observed at the promoter, first exon and first intron regions of *MAF1* chromatin in *hda5-1* mutant plants (Figure 6b). Similarly, increased levels of H3K4Me3 were also observed at the promoter and first exon regions of *FLC* chromatin in *hda5-1* mutants. The increased levels of H3K9K14Ac and H3K4Me3 are consistent with the increased expression of *FLC* and *MAF1* in *hda5-1* plants.

HDA5 interacts with FLD, FVE and HDA6

Previous studies indicated that Arabidopsis HDA6 is associated with FLD and FVE, forming HDAC complexes that control flowering time (Gu *et al.*, 2011; Yu *et al.*, 2011). We analyzed whether HDA5 also interacts with FLD and FVE by using bimolecular fluorescence complementation (BiFC) analysis. As shown in Figure 7a, HDA5 interacts with FLD and FVE in the nuclei of Arabidopsis protoplasts. Similar results were also observed using tobacco leaf epidermal cells in BiFC assays (Figure S5). In addition, HDA5 also interacts with HDA6 in BiFC assays (Figure S5).

The interaction of HDA5 with FLD and FVE was further analyzed using co-immunoprecipitation assays. Tobacco leaves were infiltrated with *Agrobacterium* cultures carrying 35S:GFP-HDA5 and 35S:Myc-FLD or 35S:Myc-FVE constructs, and leaf extracts were analyzed by co-immunoprecipitation. As shown in Figure 7b, GFP–HDA5 was co-immunoprecipitated by Myc–FLD and Myc–FVE. The interaction was specific, as GFP–HDA5 was not detected in the absence of Myc–FLD or Myc–FVE.

Genome-wide analysis of transcriptome changes in hda5 *and* hda6 *mutant plants*

Expression patterns from the public Arabidopsis microarray databases (http://www.bar.utoronto.ca/efp/cgi-bin/efpWeb.cgi) revealed that *HDA5* and *HDA6* display similar expression patterns in Arabidopsis (Figure S6). In particular, both *HDA5* and *HDA6* are highly expressed in the shoot apex, supporting roles in flower initiation. To further understand the functions of HDA5 and HDA6 in Arabidopsis, we examined transcriptome changes in *hda5* and *hda6* mutants by deep mRNA sequencing analysis. We performed transcriptomic analyses of Col-0 wild-type, *hda5-1* and *hda6* (*axe1-5*) mutant seedlings grown under LD conditions for 14 days. Genes more than twofold increased or decreased expression and a P value ≤ 0.05 for comparison of expression between the mutant and the wild-type were considered to show significant expression differences. In *hda5-1* mutant plants, 1161 genes were up-regulated and 900 genes were down-regulated (Figure 8a,b and Data S1). In comparison, 1761 genes were up-regulated and 1057 genes were down-regulated in *axe1-5* mutant plants (Figure 8a,b and Data S2). We found that more than half of the genes regulated by HDA5 [590 up-regulated genes (51%)

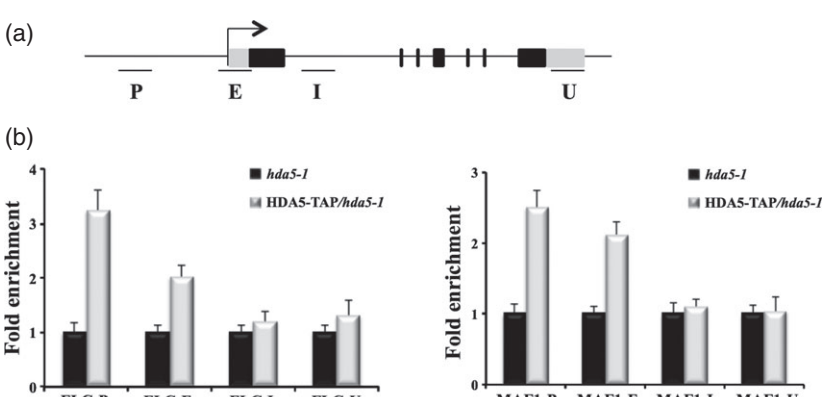

Figure 5. Direct binding of HDA5 to *FLC* and *MAF1*.
(a) Schematic structure of *FLC* clade members and the regions examined by ChIP. Exons and untranslated regions are represented by black and gray boxes, respectively. P, promoter; E, exon; I, Intron; U, UTR.
(b) ChIP analysis of HDA5-tandem affinity purification (TAP) binding to the genomic regions of *FLC* and *MAF1*. Eighteen-day-old *hda5-1* plants expressing HDA5-TAP (HDA5-TAP/*hda5-1*) were used for ChIP analysis. Fold enrichment of each fragment was calculated by normalizing the amount of target DNA fragments against the input DNA.

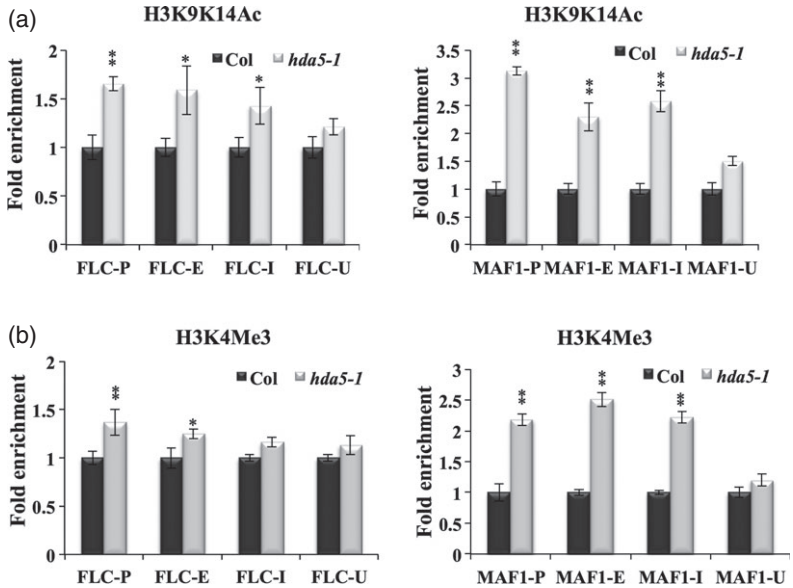

Figure 6. Histone modification levels of *FLC* and *MAF1* in *hda5-1.*
(a) Relative levels of histone H3K9K14Ac in *FLC* and *MAF1.*
(b) Relative levels of histone H3K4Me3 in *FLC* and *MAF1.*
Eighteen-day-old plants were used for ChIP analysis. The immunoprecipitated DNA was quantified by real-time PCR, and values were normalized to an internal control (ACTIN2). The fold enrichment of *hda5-1* over Col-0 is shown (means ± SD). Asterisks indicate statistically significant differences compared with Col-0 (*$P < 0.05$, **$P < 0.01$, *t* test).

and 570 down-regulated genes (63%)] were also regulated by HDA6 (Figure 8a,b and Data S3). Functional classification revealed similar patterns for HDA5- and HDA6-regulated genes (Figure 8c,d), suggesting that HDA5 and HDA6 may have similar functions in Arabidopsis.

We further performed clustering and heat map analysis of HDA5- and HDA6-regulated genes. Very similar transcriptome changes were identified when comparing *hda5* and *hda6* mutants with Col-0 wild-type plants (Figure 9a). Interestingly, features annotated as transposable elements in the heat map corresponded closely to HDA6-specific regulated genes (Figure 9a). This observation is consistent with a previous finding that HDA6 is involved in the regulation of transposable elements (To *et al.*, 2011; Yu *et al.*, 2011). In addition, the correlations between genes that were co-activated by HDA5 and HDA6 (Figure 9b) or co-repressed by HDA5 and HDA6 (Figure 9c) were analyzed by scatter plot. Genes co-regulated by HDA5 and HDA6 are indicated by black spots, whereas genes regulated by HDA5 or HDA6 alone are indicated by red and green spots, respectively (Figure 9b,c). When comparing the activated genes, a group of transposable element genes were highly expressed in the *hda6* mutant (Figures 9a and S7), but were not expressed in the *hda5-1* mutant, indicating that these transposable elements were specifically controlled by HDA6.

The functions of the differentially expressed genes were classified by examining their gene ontology (GO) (Ashburner *et al.*, 2000), and functionally clustered by using the DAVID resource (Database for Annotation, Visualization and Integrated Discovery) (Huang *et al.*, 2009). As shown in Figure 9d, GO analysis suggested that genes co-regulated by HDA5 and HDA6 are involved in various pathways, including regulation of transcription, hormone stimulus, abiotic stress, defense and cell-wall organization. These results suggest that both HDA5 and HDA6 play important roles in plant developmental processes and plant responses to environmental stresses.

DISCUSSION

Previous studies indicated that recombinant Arabidopsis HDA19 protein expressed in *E. coli* only displayed very low histone deacetylase activity *in vitro* (Fong *et al.*, 2006). In contrast, recombinant HDA6, HDA9, HDA15 and HDA17 expressed in *E. coli* did not show any HDAC enzymatic activity (Fong *et al.*, 2006; Liu *et al.*, 2013). In this study, we demonstrate that recombinant HDA5 expressed in *E. coli* displayed strong HDAC enzymatic activity, and this activity was inhibited by TSA. Furthermore, purified GFP–HDA5 protein from transgenic plants also displayed strong HDAC activity. As recombinant proteins of most Arabidopsis HDACs expressed in *E. coli* did not show measurable histone deacetylase activity, it is possible that these HDACs require the association of other cofactors or post-translational modifications for activity (Ellis *et al.*, 2008). The mutated recombinant HDA5 proteins D198A, D291A and H200A showed no histone deacetylase activity, indicating that the amino acid residues D198, D291 and H200 are critical for the enzymatic activity of HDA5. These three amino acids correspond to the residues responsible for chelating Zn^{2+} in human HDAC8 (Lombardi *et al.*, 2011), suggesting that HDA5 is a Zn^{2+}-containing enzyme.

Recent studies indicated that histone acetylation and deacetylation are involved in the control of flowering time in Arabidopsis (He *et al.*, 2003; Wu *et al.*, 2008; Yu *et al.*, 2011). Four major flowering pathways (photoperiod, vernalization, autonomous, and gibberellin pathways) have been identified in Arabidopsis (Henderson and Dean, 2004;

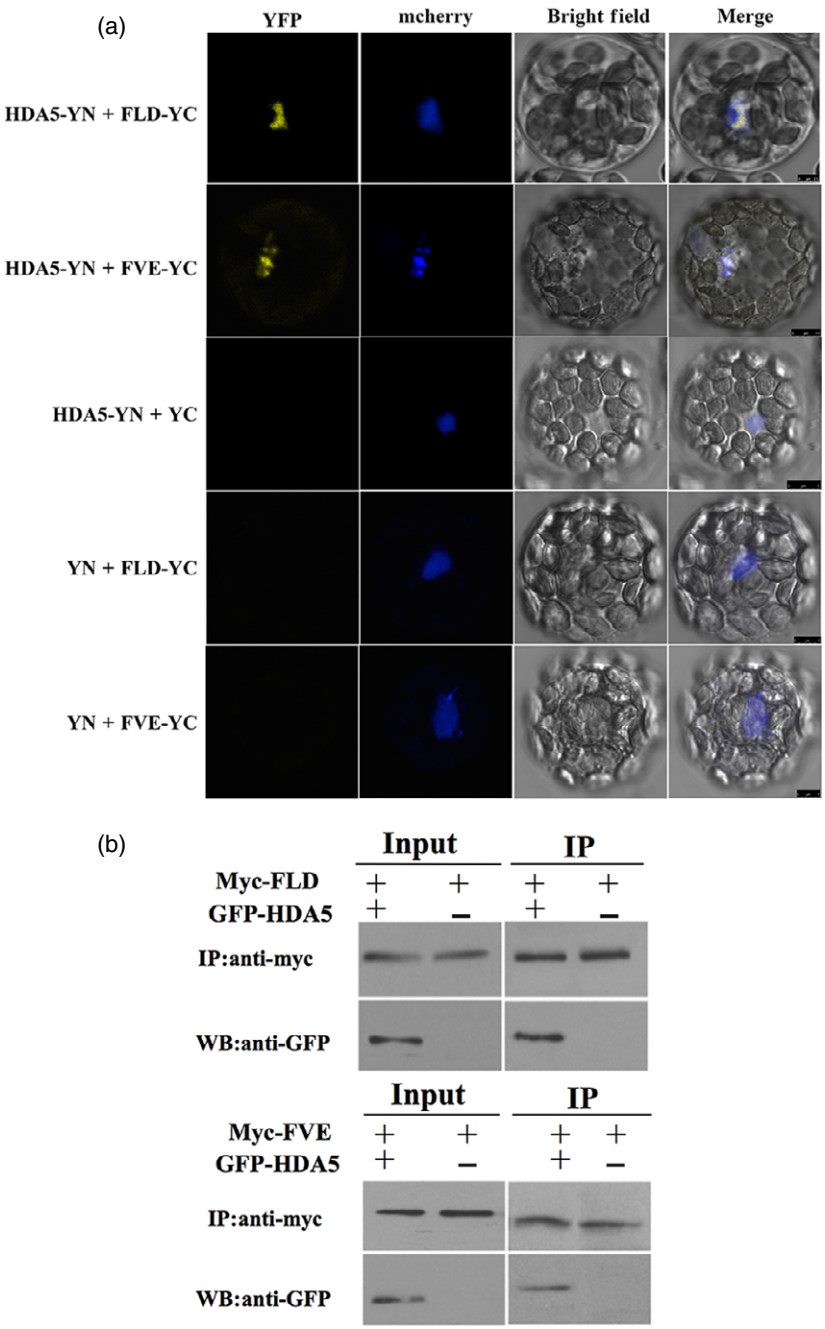

Figure 7. HDA5 physically interacts with FLD and FVE.
(a) BiFC assays in Arabidopsis protoplasts showing interaction of HDA5 with FLD and FVE in living cells.
(b) Interaction of HDA5 with FLD and FVE in co-immunoprecipitation assays. Protein extracts co-expressing 35S::GFP-HDA5 and 35S::Myc-FLD/FVE in *N. benthamiana* leaves were immunoprecipitated using anti-Myc antibody and analyzed by Western blotting.

Kim and Sung, 2014). The Arabidopsis autonomous floral-promotion pathway promotes flowering independently of the photoperiod and vernalization pathways (Michaels and Amasino, 2001). Previously, we reported that HDA6 is involved in the autonomous pathways of flowering, by repressing the expression of *FLC* (Wu *et al.*, 2008; Yu *et al.*, 2011). Similar to *hda6* mutant plants, *hda5* plants were late-flowering under both LD and SD conditions, and the delay in flowering time was completely corrected by vernalization, indicating that HDA5 is also involved in the autonomous pathway of flowering. In both *hda5* and *hda6* mutants, *FLC* was up-regulated and hyperacetylated. Similar to *hda6* mutants (Yu *et al.*, 2011), the late-flowering phenotype of *hda5* mutants is suppressed by the *flc* null mutant. These data indicate that HDA5 and HDA6 are involved in flowering by regulating *FLC* expression. In addition to *FLC*, five *FLC* homologs, *MAF1*–*MAF5*, are involved in the regulation of flowering time in Arabidopsis (Gu *et al.*, 2013). We found that the expression of *MAF1* was increased in both *hda5* and *hda6* plants, whereas the

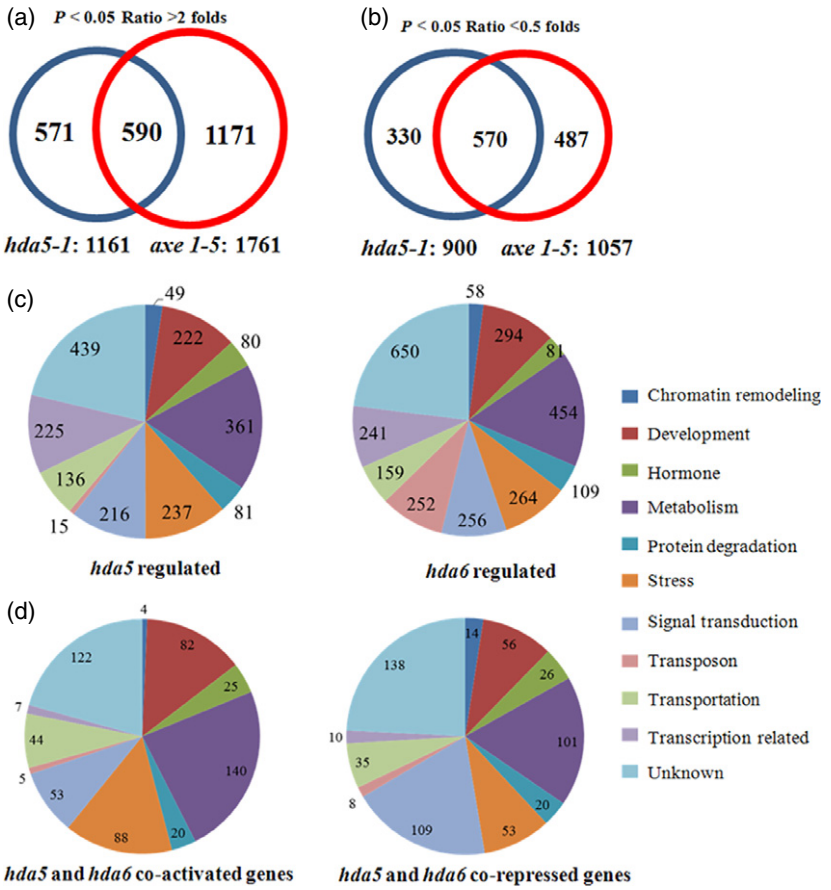

Figure 8. Genome-wide analysis of gene expression regulated by HDA5 and HDA6.
(a,b) Venn diagram of up-regulated (a) and down-regulated (b) genes specific to *hda5-1* or *hda6* (*axe1-5*) mutant plants.
(c) Functional classification of HDA5- or HDA6-regulated genes.
(d) Functional classification of co-activated or co-repressed genes in *hda5* and *hda6*.

expression of *MAF4* and *MAF5* was up-regulated only in *hda6* plants. ChIP analyses revealed that both HDA5 and HDA6 bind to *FLC* and *MAF1* chromatin. In addition, HDA6 also binds to *MAF4* and *MAF5* chromatin. These data indicate that, in addition to targeting to *FLC* and *MAF1*, HDA6 also targets *MAF4* and *MAF5*.

Transcriptome analysis using RNA-seq indicated that HDA5 and HDA6 co-regulate gene expression involved in a variety of biological processes. In addition to genes involved in flowering, genes involved in hormone stimulus, abiotic stress, defense and cell-wall organization were affected in *hda5* and *hda6* mutants, supporting the assumption that both HDA5 and HDA6 play important roles in multiple plant developmental processes and plant responses to environmental stresses. Previous studies suggested that HDA6 is required for maintaining cytosine methylation and transposon silencing by interacting with the DNA methyltransferase MET1 (To *et al.*, 2011; Liu *et al.*, 2012). A large subset of transposons were up-regulated in *hda6* plants, supporting the importance of HDA6 in maintaining the stability of transposable elements. In contrast, the expression of transposons was not affected in *hda5* mutants, indicating that HDA5 is not involved in transposon silencing.

The autonomous pathway genes, including *FLD* and *FVE*, function to repress the expression of *FLC*. FLD is a lysine-specific demethylase 1-type histone demethylase that removes methyl groups from mono- and dimethylated histone H3K4 (Jiang *et al.*, 2007; Liu *et al.*, 2007). Previously, we reported that HDA6 is associated with FLD, which is involved in the regulation of flowering time (Yu *et al.*, 2011). In this study, we found that HDA5 also directly interacts with the histone demethylase FLD. Similar to *hda6* and *fld* mutants (Yu *et al.*, 2011), increased levels of histone H3 acetylation and H3K4 trimethylation at *FLC* were also found in *hda5* plants. These results support a scenario in which cross-talk between histone deacetylation and demethylation is mediated by the physical association of FLD with HDA5 and HDA6. FVE is the Arabidopsis homolog of the human histone-binding protein RbAp46/48 (Gu *et al.*, 2011). Hyperacetylation levels were found at *FLC* chromatin in *fve* mutant plants (He *et al.*, 2003; Ausin *et al.*, 2004; Kim *et al.*, 2004), suggesting that FVE is required to deacetylate *FLC* chromatin and repress *FLC* expression. We found that FVE directly interacts with HDA5, indicating that these proteins may be part of the same protein complex. Taken together, the results suggest that

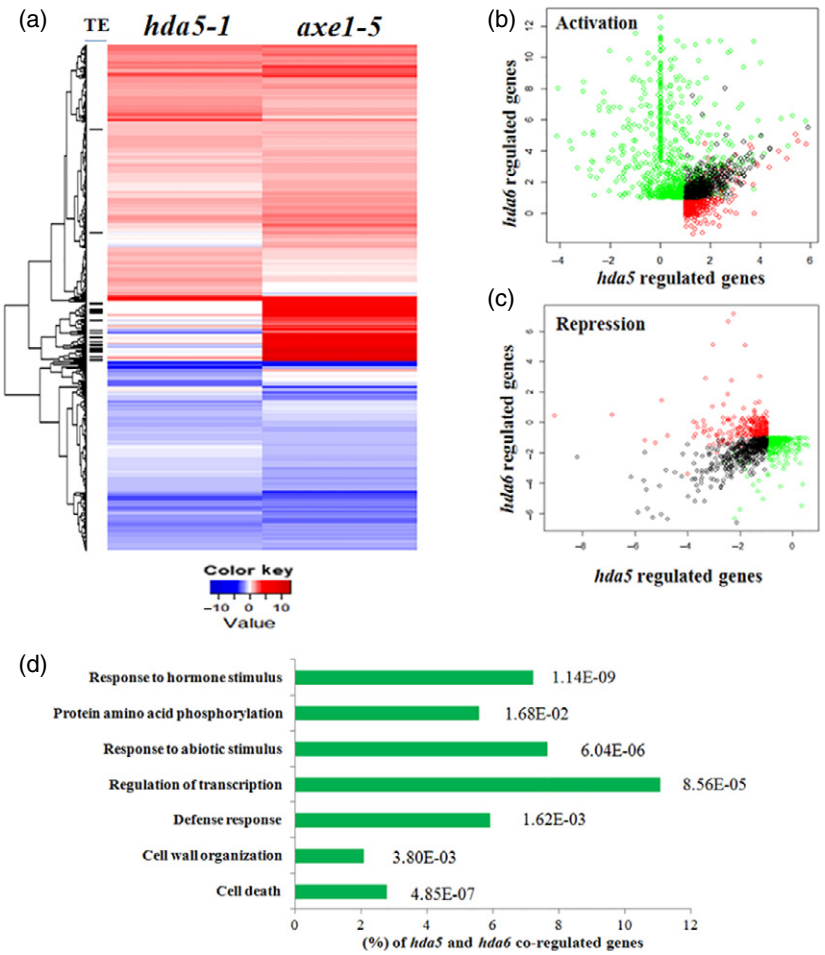

Figure 9. HDA5 and HDA6 co-regulate gene expression.
(a) Heatmap of genes affected in *hda5-1* and *axe1-5*. The bar represents the $\log_2$ ratio. TE represents transposable elements.
(b,c) Correlation $\log_2$ fold change values between genes that are up-regulated (b) or down-regulated (c) in *hda5-1* and *axe1-5*.
(d) DAVID functional clustering, showing the percentage (%) of co-regulated genes and the *P* value for highly enriched GO terms in *hda5-1* and *axe1-5*.

FLD and FVE act in a HDAC complex containing HDA5 and HDA6 to repress *FLC* expression.

We found that HDA5 interacts with HDA6 in BiFC assays, suggesting that they may form heterodimers *in vivo*. In mammalian cells, HDAC1 and HDAC2 form homo- and heterodimers, and dimer formation is a requirement for HDAC activity, as dissociation of the dimer using a HDAC1 N-terminal peptide inhibits HDAC activity (Delcuve *et al.*, 2012). The mammalian class I HDAC HDAC3 forms heterodimers with the class II HDAC HDAC4. Moreover, the Calcium/calmodulin-dependent protein kinase II (CaMKII)-dependent regulation of mammalian HDAC5 is dependent on heterodimerization with HDAC4 and formation of a complex (Backs *et al.*, 2008). Further research is required to investigate the functional significance of the heterodimer formation between HDA5 and HDA6 proteins in Arabidopsis. In mammalian cells, it has been reported that RPD3/HDA1 family HDACs are components of several multi-protein complexes such as Sin3, Mi2/NuRD, N-CoR/SMRT and CoREST (Seto and Yoshida, 2014). In addition, a large number of interacting partners of yeast and animal HDACs have been identified. In comparison, little is known regarding plant HDAC protein complexes and their interacting partners. Our study revealed that HDA5 and HDA6 form a repressor complex with FLD and FVE to regulate flowering time, indicating that plant HDACs cooperate with other chromatin and transcriptional regulators to regulate gene expression.

EXPERIMENTAL PROCEDURES

Plant materials

Arabidopsis thaliana plants were grown at 23°C under long-day conditions (LD, 16 h light/8 h dark) or short-day conditions (SD, http://www3.gehealthcare.com/ 8 h light/16 h dark). The *hda5* T-DNA mutants *hda5-1* (SALK_007503) and *hda5-2* (SALK_021241) were obtained from the Arabidopsis Information Resource Center (http://www.arabidopsis.org/).

Expression and purification of recombinant HDAC proteins in *E. coli*

Full-length HDACs and mutated HDA5 were cloned into the pGEX-4T-3 expression vector (Amersham, http://www3.gehealthcare.com/). The expression vectors were transformed into *E. coli* Rosetta, and expression of the recombinant proteins was induced by addition of 0.1 mM isopropyl-β-D-thiogalactopyranoside. Cells were harvested by centrifugation (6000 ***g***, 4°C for 10 min) and suspended in PBS. After sonication, the soluble cell extract was

applied to a GST affinity column (Novagen, https://www.novagen.com/), and recombinant proteins were purified according to the manufacturer's instructions.

Histone deacetylase enzymatic assays

HDAC assays were performed using an HDAC activity colorimetric assay kit (BioVision, https://www.biovision.com/) according to the manufacturer's instructions. Briefly, 4 μg of purified proteins was diluted to 85 μL of double-distilled H_2O in each well, and 10 μl of 10× HDAC Assay Buffer [15 mM Tris-HCl (pH 8), 250 μM EDTA, 250 μM NaCl, and 10% glycerol] and 5 μl of colorimetric substrate (10 mM Boc-Lys(Ac)-pNA) (Biovision, Catalog #K331-100) http://www.biovision.com/ were added to each well and incubated at 37°C for 1 h. The reaction was stopped by adding 10 μl of Lys developer [0.01 mg/mL Trypsin, 50 mM Tris-HCl (pH 8), 100 mM NaCl, 2 μM TSA, 30% Isopropanol] (Biovision, Catalog #K331-100) and incubating the plate at 37°C for 30 min. The HDAC activity was then measured spectrophotometrically at 405 nm. HeLa nuclear extracts (4 μg) were used as positive controls. The HDAC inhibitor TSA was used to demonstrate the specificity of deacetylation activities.

Quantitative reverse transcriptase (RT)-PCR analysis

Total RNA was isolated using TRIZOL reagent (Invitrogen, https://www.lifetechnologies.com/) according to the manufacturer's instructions. Two micrograms of total RNA were used to synthesize cDNA. Real-time PCR was performed using iQ SYBR Green Supermix solution (Bio-Rad, https://www.bio-rad.com/). The gene-specific primers used for real-time RT-PCR are listed in Table S1. Each sample was quantified at least in triplicate, and normalized by using *Ubiquitin10* (*UBQ*) as an internal control.

Chromatin immunoprecipitation assays

ChIP assays were performed as previously described (Yu *et al.*, 2011). Chromatin extracts were prepared from seedlings treated with formaldehyde. The chromatin was sheared to a mean length of 500 bp by sonication, and proteins and DNA fragments were then immunoprecipitated using antibodies against acetylated histone H3K9K14 (Millipore, https://www.merckmillipore.com/), trimethylated histone H3K4 (Millipore), Myc (Sigma, http://www.sigmaaldrich.com) or GFP (Santa Cruz Biotechnologies, http://www.scbt.com). The DNA cross-linked to immunoprecipitated proteins were reversed, and then analyzed by real-time PCR using specific primers (Table S2).

Bimolecular fluorescence complementation and co-immunoprecipitation assays

To generate the constructs for BiFC assays, full-length cDNA fragments of HDA5, HDA6, FVE and FLD were PCR-amplified and cloned into pCR8/GW/TOPO vectors (Invitrogen), and then recombined into the YN vector pEarleyGate201-YN and the YC vector pEarleyGate202-YC (Lu *et al.*, 2010). Constructed vectors were transiently transformed into Arabidopsis protoplasts and tobacco leaves (*Nicotiana benthamiana*). Transfected leaves were then examined using a TCS SP5 confocal spectral microscope imaging system (Leica, https://www.leica.com/).

Co-immunoprecipitation assays were performed as previously described (Yu *et al.*, 2011). Anti-GFP and anti-Myc were used as primary antibodies, and the resulting signals were detected using a Pierce ECL Western blotting kit (Pierce, https://www.lifetechnologies.com/).

RNA sequencing

Poly(A)-containing mRNA molecules were purified using poly(T) oligo-attached magnetic beads. The fragmentation mix of the TruSeq RNA Library Prep Kit v2 (Cat. no. RS-122-201, Illumina) was added to fragment the mRNA. cDNA was synthesized by random hexamer priming. A second strand was generated to create double-stranded cDNA. cDNA templates were purified using a the MinElute PCR Purification Kit (Qiagen, https://www.qiagen.com/), followed by end repair, poly(A) tailing and adaptor connection. Libraries were sequenced using a HiSeq™ 2500 (Illumina, http://www.illumina.com/). The CASAVA pipeline (version 1.8, Illumina) was used to produces FASTQ files. The first step in the trimming process was to convert the quality score (*Q*) to error probability. Next, a new value was calculated for every base: 0.05 minus error probability. This value is negative for low-quality bases, where the error probability is high. For each base, we calculated the running sum of this value. If the sum was below zero, it was set to zero. The part of the sequence to be retained was between the first positive value of the running sum and the highest value of the running sum. Bases before and after this region were removed. In addition, reads shorter than 35 bp were discarded.

More than 21 million clean reads were obtained in each sample. All clean reads were mapped to the TAIR10 genome (http://www.arabidopsis.org/) using the following strategy. First, reads were mapped to the TAIR10 genome using Bowtie2 (Langmead and Salzberg, 2012), and only reads with a mapping identity ≥98% were accepted. The rest reads were mapped to the TAIR10 transcripts using Bowtie2 with the same identity filter, and then translocated to the genome. Finally, rest reads were mapped to the TAIR10 genome using BLAT (Kent, 2002). Values for RPKM (reads per kilobase of exon model per million mapped reads; Mortazavi *et al.*, 2008) were computed based on these mapped reads using RackJ (http://rackj.sourceforge.net/), and Student's *t*-tests were performed on RPKM values. Genes were deemed significantly differentially expressed if the *P* value was <0.05 and the relative change was more than twofold. GO terms and functionally clustered genes were analyzed using the DAVID web tools (Huang *et al.*, 2009). Both heatmap and scatter plot analyses were performed in R language (Severin *et al.*, 2010).

ACKNOWLEDGMENTS

We thank Cheng-Chieh Wu (Academia Sinica, Taipei, Taiwan) for help with analyzing RNA-sequencing data. We also thank Technology Commons, College of Life Science, National Taiwan University, for use of the Bio-Rad real-time PCR system and the confocal spectral microscope imaging system. This work was supported by the National Science Council of Taiwan (101-2311-B-002-012-MY3 and 103-2321-B-002-039), the National Taiwan University (104R892005) and the Academia Sinica (AS-1102-TP-B05). This work was also supported by the National Basic Research Program of China (973 program, grant number 2012CB910900), the National Natural Science Foundation of China (31371308 and 31200965), the China Postdoctoral Science Foundation (2014M562220) and the Guangdong Natural Science Foundation (S2012040006474).

SUPPORTING INFORMATION

Additional Supporting Information may be found in the online version of this article.

Figure S1. Phenotypes of *hda5-1*, *fve and hda5-1*/*fve* double mutants.

Figure S2. *FLC*- and *MAF1*-dependent late flowering in *hda5-1*.

Figure S3. Complementation of the late-flowering phenotype of *hda5-1* by over-expression of *35S:HDA5-TAP*.

Figure S4. Direct binding of HDA6 to *FLC* clade members.

Figure S5. HDA5 interacts with FLD, FVE and HDA6 in *N. benthamiana* leaves.

Figure S6. Heatmap analysis of *HDA5* and *HDA6* expression at various developmental stages.

Figure S7. HDA6 is responsible for maintaining the stability of transposable elements.

Data S1. Up-regulated and down-regulated genes in *hda5-1* mutant plants.

Data S2. Up-regulated and down-regulated genes in *axe1-5* mutant plants.

Data S3. Genes co-regulated by HDA5 and HDA6.

Table S1. Gene-specific primer pairs for quantitative RT-PCR analyses.

Table S2. Primers used for quantitative PCR analyses in ChIP assays.

REFERENCES

Alinsug, M.V., Yu, C.W. and Wu, K. (2009) Phylogenetic analysis, subcellular localization, and expression patterns of RPD3/HDA1 family histone deacetylases in plants. *BMC Plant Biol.* **9**, 37.

Ashburner, M., Ball, C.A., Blake, J.A., Botstein, D., Butler, H., Cherry, J.M., Davis, A.P., Dolinski, K., Dwight, S.S. and Eppig, J.T. (2000) Gene ontology: tool for the unification of biology. *Nat. Genet.* **25**, 25–29.

Aufsatz, W., Mette, M.F., van der Winden, J., Matzke, M. and Matzke, A.J. (2002) HDA6, a putative histone deacetylase needed to enhance DNA methylation induced by double-stranded RNA. *EMBO J.* **21**, 6832–6841.

Ausin, I., Alonso-Blanco, C., Jarillo, J.A., Ruiz-Garcia, L. and Martinez-Zapater, J.M. (2004) Regulation of flowering time by FVE, a retinoblastoma-associated protein. *Nat. Genet.* **36**, 162–166.

Backs, J., Backs, T., Bezprozvannaya, S., McKinsey, T.A. and Olson, E.N. (2008) Histone deacetylase 5 acquires calcium/calmodulin-dependent kinase II responsiveness by oligomerization with histone deacetylase 4. *Mol. Cell. Biol.* **28**, 3437–3445.

Berger, S.L. (2007) The complex language of chromatin regulation during transcription. *Nature*, **447**, 407–412.

Delcuve, G.P., Khan, D.H. and Davie, J.R. (2012) Roles of histone deacetylases in epigenetic regulation: emerging paradigms from studies with inhibitors. *Clin. Epigenetics*, **12**, 5.

Ellis, D.J., Yuan, Z. and Seto, E. (2008) Determination of protein lysine deacetylation. *Curr. Protoc. Protein Sci.* Chapter 14, Unit 14.12. 1–14. doi: 10.1002/0471140864.ps1 412s54.

Fong, P.M., Tian, L. and Chen, Z.J. (2006) *Arabidopsis thaliana* histone deacetylase 1 (AtHD1) is localized in euchromatic regions and demonstrates histone deacetylase activity *in vitro*. *Cell Res.* **16**, 479–488.

Gu, X., Jiang, D., Yang, W., Jacob, Y., Michaels, S.D. and He, Y. (2011) Arabidopsis homologs of retinoblastoma-associated protein 46/48 associate with a histone deacetylase to act redundantly in chromatin silencing. *PLoS Genet.* **7**, e1002366.

Gu, X., Le, C., Wang, Y., Li, Z., Jiang, D. and He, Y. (2013) Arabidopsis FLC clade members form flowering-repressor complexes coordinating responses to endogenous and environmental cues. *Nat. Commun.* **4**, 1947.

He, Y., Michaels, S.D. and Amasino, R.M. (2003) Regulation of flowering time by histone acetylation in Arabidopsis. *Science*, **302**, 1751–1754.

Henderson, I.R. and Dean, C. (2004) Control of Arabidopsis flowering: the chill before the bloom. *Development*, **131**, 3829–3838.

Hollender, C. and Liu, Z. (2008) Histone deacetylase genes in Arabidopsis development. *J. Integr. Plant Biol.* **50**, 875–885.

Huang, D.W., Sherman, B.T. and Lempicki, R.A. (2009) Systematic and integrative analysis of large gene lists using DAVID bioinformatics resources. *Nat. Protoc.* **4**, 44–57.

Ietswaart, R., Wu, Z. and Dean, C. (2012) Flowering time control: another window to the connection between antisense RNA and chromatin. *Trends Genet.* **28**, 445–453.

Jiang, D., Yang, W., He, Y. and Amasino, R.M. (2007) Arabidopsis relatives of the human lysine-specific demethylase1 repress the expression of FWA and FLOWERING LOCUS C and thus promote the floral transition. *Plant cell*, **19**, 2975–2987.

Kent, W.J. (2002) BLAT – the BLAST-like alignment tool. *Genome Res.* **12**, 656–664.

Kim, H.J., Hyun, Y., Park, J.Y., Park, M.J., Park, M.K., Kim, M.D., Kim, H.J., Lee, M.H., Moon, J. and Lee, I. (2004) A genetic link between cold responses and flowering time through FVE in *Arabidopsis thaliana*. *Nat. Genet.* **36**, 167–171.

Kim, D.H. and Sung, S. (2014) Genetic and epigenetic mechanisms underlying vernalization. *Arabidopsis Book*, **12**, e0171.

Krogan, N.T., Hogan, K. and Long, J.A. (2012) APETALA2 negatively regulates multiple floral organ identity genes in Arabidopsis by recruiting the co-repressor TOPLESS and the histone deacetylase HDA19. *Development*, **139**, 4180–4190.

Langmead, B. and Salzberg, S. (2012) Fast gapped-read alignment with Bowtie 2. *Nat. Methods*, **9**, 357–359.

Liu, F., Quesada, V., Crevillen, P., Baurle, I., Swiezewski, S. and Dean, C. (2007) The Arabidopsis RNA-binding protein FCA requires a lysine-specific demethylase 1 homolog to downregulate FLC. *Mol. Cell*, **28**, 398–407.

Liu, F., Marquardt, S., Lister, C., Swiezewski, S. and Dean, C. (2010) Targeted 3′ processing of antisense transcripts triggers Arabidopsis FLC chromatin silencing. *Science*, **327**, 94–97.

Liu, X., Yu, C.W., Duan, J., Luo, M., Wang, K., Tian, G., Cui, Y. and Wu, K. (2012) HDA6 directly interacts with DNA methyltransferase MET1 and maintains transposable element silencing in Arabidopsis. *Plant Physiol.* **158**, 119–129.

Liu, X., Chen, C.Y., Wang, K.C. *et al.* (2013) PHYTOCHROME INTERACTING FACTOR3 associates with the histone deacetylase HDA15 in repression of chlorophyll biosynthesis and photosynthesis in etiolated Arabidopsis seedlings. *Plant Cell*, **25**, 1258–1273.

Liu, X., Yang, S., Zhao, M., Luo, M., Yu, C.W., Chen, C., Tai, R. and Wu, K. (2014) Transcriptional repression by histone deacetylases in plants. *Mol. Plant*, **7**, 764–772.

Lombardi, P.M., Cole, K.E., Dowling, D.P. and Christianson, D.W. (2011) Structure, mechanism, and inhibition of histone deacetylases and related metalloenzymes. *Curr. Opin. Struct. Biol.* **21**, 735–743.

Long, J.A., Ohno, C., Smith, Z.R. and Meyerowitz, E.M. (2006) TOPLESS regulates apical embryonic fate in Arabidopsis. *Science*, **312**, 1520–1523.

Luo, M., Yu, C.W., Chen, F.F., Zhao, L., Tian, G., Liu, X., Cui, Y., Yang, J.Y. and Wu, K. (2012) Histone deacetylase HDA6 is functionally associated with AS1 in repression of KNOX genes in arabidopsis. *PLoS Genet.* **8**, e1003114.

Lu, Q., Tang, X., Tian, G., Wang, F., Liu, K., Nguyen, V., Kohalmi, S.E., Keller, W.A., Tsang, E.W., Harada, J.J., Rothstein, S.J. and Cui, Y. (2010) Arabidopsis homolog of the yeast TREX-2 mRNA export complex: components and anchoring nucleoporin. *Plant J.* **61**, 259–270.

Marquardt, S., Raitskin, O., Wu, Z., Liu, F., Sun, Q. and Dean, C. (2014) Functional consequences of splicing of the antisense transcript COOLAIR on FLC transcription. *Mol. Cell*, **54**, 156–165.

Michaels, S.D. and Amasino, R.M. (1999) FLOWERING LOCUS C encodes a novel MADS domain protein that acts as a repressor of flowering. *Plant Cell*, **11**, 949–956.

Michaels, S.D., Bezerra, I.C. and Amasino, R.M. (2004) FRIGIDA-related genes are required for the winter-annual habit in Arabidopsis. *Proc. Natl Acad. Sci. USA*, **101**, 3281–3285.

Michaels, S.D. and Amasino, R.M. (2001) Loss of FLOWERING LOCUS C activity eliminates the late-flowering phenotype of FRIGIDA and autonomous pathway mutations but not responsiveness to vernalization. *Plant Cell*, **13**, 935–941.

Mortazavi, A., Williams, B.A., McCue, K., Schaeffer, L. and Wold, B. (2008) Mapping and quantifying mammalian transcriptomes by RNA-Seq. *Nat. Methods*, **5**, 621–628.

Ratcliffe, O.J., Kumimoto, R.W., Wong, B.J. and Riechmann, J.L. (2003) Analysis of the Arabidopsis MADS AFFECTING FLOWERING gene family: MAF2 prevents vernalization by short periods of cold. *Plant Cell*, **15**, 1159–1169.

Rubio, V., Shen, Y., Saijo, Y., Liu, Y., Gusmaroli, G., Dinesh-Kumar, S.P. and Deng, X.W. (2005) An alternative tandem affinity purification strategy applied to Arabidopsis protein complex isolation. *Plant J.* **41**, 767–778.

Scortecci, K.C., Michaels, S.D. and Amasino, R.M. (2001) Identification of a MADS-box gene, FLOWERING LOCUS M, that represses flowering. *Plant J.* **26**, 229–236.

Seto, E. and Yoshida, M. (2014) Erasers of histone acetylation: the histone deacetylase enzymes. *Cold Spring Harb. Perspect. Biol.* **6**, a018713.

Severin, A.J., Woody, J.L., Bolon, Y.-T., Joseph, B., Diers, B.W., Farmer, A.D., Muehlbauer, G.J., Nelson, R.T., Grant, D. and Specht, J.E. (2010) RNA-Seq Atlas of *Glycine max*: a guide to the soybean transcriptome. *BMC Plant Biol.* **10**, 160.

Tian, L. and Chen, Z.J. (2001) Blocking histone deacetylation in *Arabidopsis* induces pleiotropic effects on plant gene regulation and development. *Proc. Natl Acad. Sci. USA*, **98**, 200–205.

To, T.K., Kim, J.M., Matsui, A. *et al.* (2011) Arabidopsis HDA6 regulates locus-directed heterochromatin silencing in cooperation with MET1. *PLoS Genet.* **7**, e1002055.

Vannini, A., Volpari, C., Filocamo, G. *et al.* (2004) Crystal structure of a eukaryotic zinc-dependent histone deacetylase, human HDAC8, complexed with a hydroxamic acid inhibitor. *Proc. Natl Acad. Sci. USA*, **101**, 15064–15069.

Wang, L., Kim, J. and Somers, D.E. (2013) Transcriptional corepressor TOPLESS complexes with pseudoresponse regulator proteins and histone deacetylases to regulate circadian transcription. *Proc. Natl Acad. Sci. USA*, **110**, 761–766.

Wang, Z.W., Wu, Z., Raitskin, O., Sun, Q.W. and Dean, C. (2014) Antisense-mediated FLC transcriptional repression requires the P-TEFb transcription elongation factor. *Proc. Natl Acad. Sci. USA*, **111**, 7468–7473.

Wu, K., Zhang, L., Zhou, C., Yu, C.W. and Chaikam, V. (2008) HDA6 is required for jasmonate response, senescence and flowering in Arabidopsis. *J. Exp. Bot.* **59**, 225–234.

Yang, X.J. and Seto, E.Y. (2007) HATs and HDACs: from structure, function and regulation to novel strategies for therapy and prevention. *Oncogene*, **26**, 5310–5318.

Yu, C.W., Liu, X., Luo, M., Chen, C., Lin, X., Tian, G., Lu, Q., Cui, Y. and Wu, K. (2011) HISTONE DEACETYLASE6 interacts with FLOWERING LOCUS D and regulates flowering in Arabidopsis. *Plant Physiol.* **156**, 173–184.

Zhou, Y., Tan, B., Luo, M. *et al.* (2013) HISTONE DEACETYLASE19 interacts with HSL1 and participates in the repression of seed maturation genes in Arabidopsis seedlings. *Plant Cell*, **25**, 134–148.